World Academy of Science, Engineering and Technology
International Journal of Materials and Metallurgical Engineering
Vol:17, No:9, 2023

Thermoelectric Properties of Doped Polycrystalline Silicon Film

Li Long, Thomas Ortlepp

Abstract—The transport properties of carriers in polycrystalline silicon film affect the performance of polycrystalline silicon-based devices. They depend strongly on the grain structure, grain boundary trap properties and doping concentration, which in turn are determined by the film deposition and processing conditions. Based on the properties of charge carriers, phonons, grain boundaries and their interactions, the thermoelectric properties of polycrystalline silicon are analyzed with the relaxation time approximation of the Boltzmann transport equation. With this approach, thermal conductivity, electrical conductivity and Seebeck coefficient as a function of grain size, trap properties and doping concentration can be determined. Experiment on heavily doped polycrystalline silicon is carried out and measurement results are compared with the model.

Keywords—conductivity, polycrystalline silicon, relaxation time approximation, Seebeck coefficient, thermoelectric property.

I. Introduction

THE thermoelectric effect is widely used for the infrared radiation detection and thermoelectric generator. A lot of effort has been put into improving the performance of thermoelectric based devices. Polycrystalline silicon produced with thermal chemical vapor deposition possesses good thermoelectric properties. The structural and thermoelectric properties of polycrystalline silicon depend strongly upon the deposition conditions and process parameters. In this paper, an approach to study the thermoelectric properties of polycrystalline semiconductors on a microscopic level is developed and, thus, a model to improve the performance based on the optimization of processing parameters can be provided.

The carrier's transport in polycrystalline silicon based thermoelectric devices can be regarded as a thermodynamic system out of equilibrium, for which there is an Onsager reciprocal relation between flows and driving forces [1]. The transport coefficients, namely electrical conductivity, thermal conductivity and Seebeck coefficient, are therefore correlated and determined by the microscopic scattering of phonons and charge carriers [2]. Over the last years, a lot of research into the thermoelectric properties of semiconductor materials has been carried out. For crystalline silicon as thermoelectric conversion material, the power factor as a function of strain has been investigated with electronic structure calculations combined with the Boltzmann transport equation [3]. For polycrystalline silicon, the electronic transport (resistivity) was investigated with the thermionic emission and thermionic field emission model based on a grain boundary model [4], [5]. The grain boundary trap induced depletion zone and potential barrier were taken into account, but the phonon and ionized impurity scatterings were incorporated in the resistivity of crystalline silicon as a given parameter [4], [5]. In papers [6], [7], and [8] resistivity and Seebeck coefficient are investigated simultaneously. The phonon, ionized impurity and grain boundary scattering are incorporated, but the grain boundary traps induced carrier concentration reduction is not quantitatively incorporated.

In this paper, the relaxation time approximation of Boltzmann transport equation is used to describe the carrier's transport in polycrystalline silicon film since the system is in a near-equilibrium state [9]. The polycrystalline silicon is also modeled as crystalline silicon combined with grain boundaries. The thermal field electron emission model [4], [10] and energy filtering model of potential barrier [6], [11] are combined to provide a consistent model for polycrystaline silicon film in the frame of relaxation time approximation. For the crystallite, the different scattering mechanisms for charge carrier transport (Section II-A) are taken into account. For polycrystalline silicon, there is additional scattering due to grain boundaries. Defects caused by incomplete atomic bonding and disordered material in the grain boundary result in trapping states, which reduce the number of carriers and create space charge regions in the crystalline grains [4]. The grain boundary potential barrier and the depletion zone induced potential barrier scatter the carriers. For charge carrier scattering at grain boundaries and traps in polycrystalline silicon, the energy filtering model of nanocrytallite in [7] is extended to include these potential barriers. The effect of the boundary trap ionization induced carrier concentration reduction [4] is consistently incorporated. Further, transmission probability model of grain boundary trapping proposed in [4] is extended to the relaxation time model (Section II-B4) [11].

The theoretical approach and scattering mechanisms are shown in Section II. The extended scattering model of carriers at the grain boundary is presented in Section II-B4. The discussion and fitting of semi-empirical parameters for carrier scattering in crystalline silicon are detailed in Section II-C. Experiment approach for the preparation and measurement of heavily phosphorus and boron doped polycrystalline silicon film is described in Section III. The model is applied to experiment data of polycrystalline silicon in Section IV and discussed in Section V. Finally, the approach is summarized in Section VI.

This research was supported by a BMWI project of grant No. 49MF190037.

Li Long and Thomas Ortlepp are with CiS Forschungsinstitut für Mikrosensorik GmbH, Konrad-Zuse-Str. 14, D-99099 Erfurt, Germany (*corresponding author, e-mail: llong@cismst.de, tortlepp@cismst.de).

II. Theoretical Approach and Physical Model

In an ideal solid state lattice, the charge carriers transport losslessly. Scattering at imperfections induces nonequilibrium distribution of charge carriers that hinder the carrier's transport. The evolution of distribution function obeys the Boltzmann equation, which is a nonlinear differential equation. For small driving forces, which are the case for most of the regime interesting for the thermoelectric application, a near-equilibrium solution can be obtained by using the relaxation time approximation. In the following, the relaxation time approximation of the semiclassical description of charge carrier scattering is therefore applied to the transport problem.

A. Transport Properties of Charge Carriers in Semiconductors

In semiconductors, the charge carriers are electrons and holes. In the following, the formalism for n-type semiconductors is presented. For p-type semiconductors, the formalism can be derived in a similar manner by replacing electrons with holes. To simplify numerical calculations, the single isotropic parabolic energy band approximation is used for the electrons. The equilibrium distribution of electrons $f^0(\mathbf{k})$ observes a Fermi-Dirac distribution [3]

$$f^0(\mathbf{k}) = \frac{1}{\exp\frac{E(\mathbf{k})-\mu(T)}{kT}+1} \tag{1}$$

where $\mathbf{k}$ is the wave vector, $E(\mathbf{k})$ the energy of electrons, k is Boltzmann constant, and $\mu(T)$ the electrochemical potential of the system at temperature T. For small thermal and electrical driving forces, the distribution function of electrons $f(\mathbf{k})$ can be obtained from the relaxation time approximation of the Boltzmann equation

$$\frac{\partial f(\mathbf{k})}{\partial t} = -\frac{f(\mathbf{k})-f^0(\mathbf{k})}{\tau(\mathbf{k})} \tag{2}$$

where $\tau(\mathbf{k})$ is the relaxation time of electron with wave vector $\mathbf{k}$. As a simplification, single band effective mass approximation of electrons is used. Transport functions $L^{(n)}$ are defined as [9], [12], [1]

$$L^{(n)}(\xi,T) = 16\pi T\frac{\sqrt{2m_e^*}}{h^3}(kT)^{n+1.5} \cdot\int_0^\infty \tau(x,T)\frac{x^{1.5}(x-\xi)^n}{2(ch(x-\xi)+1)}dx \tag{3}$$

where $\xi = \frac{\mu(T)}{kT}$ is the reduced electrochemical potential, τ is the relaxation time of electron scattering by imperfections, m_e^* is the effective mass of electrons, h is Planck's constant and $x = \frac{E}{kT}$ is the reduced electron energy. Transport properties can be expressed as these transport functions $L^{(n)}$ with $n = 0$, 1 and 2. The electrical conductivity is

$$\sigma = \frac{q^2}{T}L^{(0)} \tag{4}$$

The Seebeck coefficient is

$$\alpha = -\frac{L^{(1)}}{qTL^{(0)}} \tag{5}$$

and the thermal conductivity due to charge carriers is

$$\kappa_J = \frac{1}{T^2}\left(\frac{L^{(0)}L^{(2)}-L^{(1)}L^{(1)}}{L^{(0)}}\right) \tag{6}$$

B. Scattering Processes of Charge Carriers in Silicon

Because various kinds of imperfection scattering contribute to the carrier's transport independently, their contributions to the total relaxation time obey Matthiessen's rule

$$\tau^{-1} = \sum_i \tau_i^{-1} \tag{7}$$

where the suffix i refers to the different carrier scattering processes [13]. In the following, the relaxation times for each scattering mechanism are presented for electrons in n-type silicon. For p-type silicon, similar formulas can be obtained for holes when replacing electrons with holes and the bottom edge of the conduction band with the top edge of the valence band. The effect of surface scattering is neglected because it will only be significant at very low temperatures.

1) Ionized Impurity Scattering: The Brooks-Herring formula of screening potential approximation is extended for the relaxation time for the scattering at ionized impurities [13],

$$\frac{1}{\tau_I} = a_1\frac{q^4N}{16\pi\sqrt{2m_e^*}\epsilon_0^2\epsilon_s^2E^{3/2}}f_n\left(a_2\frac{8m_e^*E\epsilon_0\epsilon_skT}{\hbar^2q^2N_D}\right) \tag{8}$$

with

$$f_n(x) = \log(1+x) - \frac{x}{1+x}$$

where $N = N_D + N_A$ is the total concentration of ionized impurities, N_D and N_A are the ionized donor and acceptor concentrations, respectively, $m_e^* = 0.26m_0$ is the effective mass of electrons (the effective mass of holes is $m_h^* = 0.36m_0$), with m_0 being the electron rest mass [14]. ϵ_0 and ϵ_s are the vacuum and silicon dielectric constants, respectively. E is the free electron energy. Here a_1 and a_2 are introduced as fitting parameters to fit the experiment results.

2) Acoustic Phonon Scattering: Under the elastic scattering approximation, the relaxation time of acoustic scattering can be expressed as

$$\frac{1}{\tau_A} = b\frac{m_e^{*3/2}kTE_{cl}^2\sqrt{2E}}{\pi\hbar^4c_l} \tag{9}$$

where the deformation potential is $E_{cl} = 9.5\,eV$ for electrons and $E_{cl} = 5\,eV$ for holes [15], the elastic constant is $c_l = 1.66\times10^{11}\,Pa$ [16], and b is a fitting parameter.

3) Optical Phonon Scattering: For silicon the carrier scattering by optical phonons is due to optical deformation potential scattering, the relaxation time is [15]

$$\frac{1}{\tau_O} = \frac{\pi c_1D_o^2}{2\rho c_2\omega_o}(n_o+\frac{1}{2}\mp\frac{1}{2})g_c(E\pm\hbar c_2\omega_o) \tag{10}$$

where $\hbar\omega_o = 63\,meV$ is the optical phonon frequency, $\rho = 2.33\,g/cm^3$ the mass density of silicon crystal [16], c_1 and c_2 are fitting parameters, and g_c the density of state function, which is [15]

$$g_c(E) = \frac{(2m_e^*)^{3/2}}{2\pi^2\hbar^3}E^{1/2} \tag{11}$$

4) Grain Boundary Scattering: Due to the highly stochastic grain distribution, scattering at different grains is incoherent and independent. As an approximation, the mean grain size d is used to represent the real grain size distribution. The grain boundaries are modeled with a very thin layer of thickness b [5], which has an areal trap density Q_t with an energy level e_t. As default parameters, a trap energy position (e_t) of $0.42\,eV$ below the conduction band edge [17] is used for n-type polycrystalline silicon (whereas for p-type polycrystalline silicon the trap energy position is $0.38\,eV$ [4], [10] above the valence band edge). The density of ionized traps in n-type polycrystalline silicon is

$$Q_t^- = \frac{Q_t}{1+2\exp\left((e_t-\mu)/(kT)\right)} \tag{12}$$

These ionized boundary traps will build a depletion zone in the grain with depletion thickness w (Fig. 1). These build up a potential barrier of height E_b at the grain boundary.

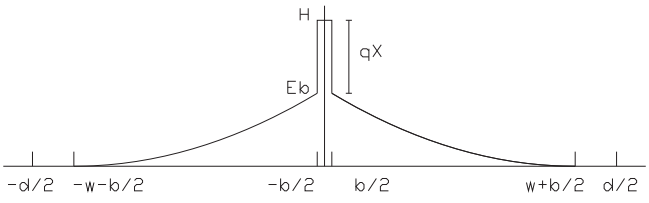

Fig. 1 The conduction band edge of the electron energy band diagram at a grain boundary in n-doped silicon

The total potential distribution is caused by the grain boundary potential barrier as well as the charged grain boundary traps induced potential barrier E_b. It can be approximated by [10]

$$V(x)=\begin{cases} V_b+\chi=\frac{H}{q} & |x|\le\frac{b}{2} \\ V_b(1-\frac{|x|-b/2}{w})^2 & \frac{b}{2}<|x|\le w+\frac{b}{2} \\ 0 & w+\frac{b}{2}<|x|\le\frac{d}{2} \end{cases} \tag{13}$$

where χ is the potential barrier height due to grain boundary, and H the total potential barrier height. The potential barrier width is supposed to be $b=2\,nm$. For the case of n-type doped semiconductors

$$V_b=-\frac{qN_Dw^2}{\epsilon_0\epsilon_s} \tag{14}$$

Depending on the trap density at the grain boundary and the grain size, there is a doping concentration N^* for which the grains are totally depleted if $N_D\le N^*$, whereas the grains are only partially depleted otherwise [4]. The potential barrier formed due to the depletion zone is

$$E_b=\begin{cases} \frac{q^2d^2}{8\epsilon_0\epsilon_s}N_D & dN_D\le N^* \\ \frac{q^2w^2}{2\epsilon_0\epsilon_s}N_D & dN_D>N^* \end{cases} \tag{15}$$

It can be assumed that the trap level is located at a constant position ϵ_t with respect to the bended conduction band edge, this results in

$$e_t=\epsilon_t-qV(x) \tag{16}$$

Under the condition of charge neutrality, one obtains

$$2wN_D=\frac{Q_t}{1+2\exp\left((\epsilon_t-\mu-qV_b)/(kT)\right)} \tag{17}$$

Possible trap centers within grains are neglected, which is reasonable for modern processing techniques (and considering the gettering effect of grain boundaries). The values for N^*, μ and w are determined with the approach in [4].

Based on the one-dimensional time-independent Wentzel-Kramer-Brillouin approximation, the transmission probability of a charge carrier of energy E through the grain boundary and the barrier $V(x)$ is [10]

$$\begin{aligned} T(E) &= \exp\left(-\frac{E_b}{E_{00}}[(1+\frac{q|\chi|}{E_b}-\alpha)^{1/2}\frac{b}{w}+y(\alpha)]\right);\ \ E\le E_b \\ &= \exp\left(-\frac{E_b}{E_{00}}[(1+\frac{q|\chi|}{E_b}-\alpha)^{1/2}\frac{b}{w}]\right);\ \ E_b<E\le H \\ &= 1;\ \ E>H \end{aligned} \tag{18}$$

where

$$\alpha=\frac{E}{E_b}$$

$$E_{00}=\frac{qh}{8\pi}\sqrt{\frac{N_D}{m_e^*\epsilon_0\epsilon_s}}$$

$$y(\alpha)=(1-\alpha)^{1/2}+\alpha\log\left[(1-\sqrt{1-\alpha})/\sqrt{\alpha}\right]$$

The average free path $\lambda_g(E)$ due to the scattering at grain boundaries can be approximated by [11]

$$\frac{1}{\lambda_g(E)}=\frac{1}{d}\frac{1-T(E)}{T(E)} \tag{19}$$

By assuming the associated relaxation time as

$$\frac{1}{\tau_g}=\sqrt{\frac{2E}{m_e^*}}\frac{1}{\lambda_g(E)} \tag{20}$$

the transmission probability model of carrier scattering at the grain and traps is generalized to the relaxation time model. The grain boundary potential barrier reduces the relaxation time especially strong for low energy charge carrier. This reduces the conductivity directly and increases the Seebeck coefficient indirectly, because $L^{(0)}$ reduces with respect to potential barrier faster than $L^{(1)}$. The depletion effect of grain boundary traps is consistently taken into account. Further, Fermi-Dirac statistics is used for carrier statistics.

C. Model Parameters for the Scattering of Charge Carriers

The thermoelectric properties of polycrystalline silicon are determined by scatterings at lattice, impurities and grain boundaries. The contribution of scatterings at lattice and impurities should be approximately the same for both crystalline and polycrystalline silicon. The relaxation time formulas of different scattering mechanisms presented in Section II-A were derived under the assumption of a single isotropic parabolic energy band for electrons and holes. One can expect that these formulas predict a qualitatively correct behavior. The parameters in (8), (9) and (10) are introduced

to quantitatively simulate the carrier scattering processes. The experimentally determined carrier mobility of crystalline silicon is therefore used to fit these parameters. To simplify the analysis, temperatures range from $260\,K$ to $360\,K$ are fitted and used for the simulations presented in this work. This is a reasonable approach because, on the one hand, polycrystalline silicon based devices are mostly used in this temperature range and, on the other hand, some scattering mechanisms can be reasonably neglected. Further, full ionization of doping is supposed [18], and Fermi-Dirac statistics is used. By fitting the experimental mobility temperature dependence at different doping concentration [19], the parameters for ionized impurity scattering are determined as $a_1 = 2.3$ and $a_2 = 3.1$ for n-type silicon, and $a_1 = 16$ and $a_2 = 1.4$ for p-type silicon. For acoustic phonon scattering, the parameters are fitted to be $b = 0.16$ for n-type silicon and $b = 6.5$ for p-type silicon. For optical phonon scattering, the parameters are fitted to be $c_1 = 100$ and $c_2 = 2.3$ for n-type silicon and $c_1 = 100$ and $c_2 = 1.5$ for p-type silicon. Further, the optical deformation potential $D_o = 9 \times 10^8\, eV/cm$ from [20] are used.

For silicon, the fitted results (Fig. 2) agree well with the experimental data (shown as symbols) [19]. This shows that carrier transport can be properly described by the relaxation time approximation of the semiclassical Boltzmann transport equation.

III. Experiment

The 4-inch n-type silicon substrate wafers are sequentially thermal oxidized with $300\,nm$ silicon dioxide, and CVD deposited $100\,nm$ nitride film and $75\,nm$ silicon dioxide film. Polycrystalline silicon film of thickness $430\,nm$ (sample a) and $300\,nm$ (sample b) are thermally deposited ($600°C$) on top of these multiple dielectric film deposited wafers. As a complement to reported experiments on doped polycrystalline silicon [10], [6], high doping concentrations are realized in this study. The sample a is doped with phosphorus oxychloride ($POCl_3$) deposition $40\,min.$ by $900°C$ and annealed thereafter $90\,min.$ at $1110°C$ in nitrogen gas. The sample b is thermally oxidized with $20\,nm$ silicon dioxide, afterward boron implant is made with implant energy $50\,keV$ and implant dose of $7 \times 10^{15}\,cm^{-2}$. After implanting, it is annealed $30\,min.$ at $1100°C$ in nitrogen gas. With photolithographical patterning doped polycrystalline silicon film are structured as Kelvin structures for electrical characterization. Contact pads are formed with $500\,nm$ Aluminum (contained 1.2% Silicon). With the full process flow the doping concentration are determined with software Silvaco [21]. The doping concentration of sample a is $1.3 \times 10^{20}\,cm^{-3}$ phosphorus, that of sample b is $6.7 \times 10^{19}\,cm^{-3}$ boron. The electrical conductivity is measured on Kelvin structures at temperature ranging from $-40°C$ to $140°C$. The test results are shown in Fig. 5. It can be seen that with this approach high doping concentration and high electrical conductivity are realized. Scanning electron microscope measurement (SEM) shows that the grain sizes are from $100\,nm$ to $200\,nm$.

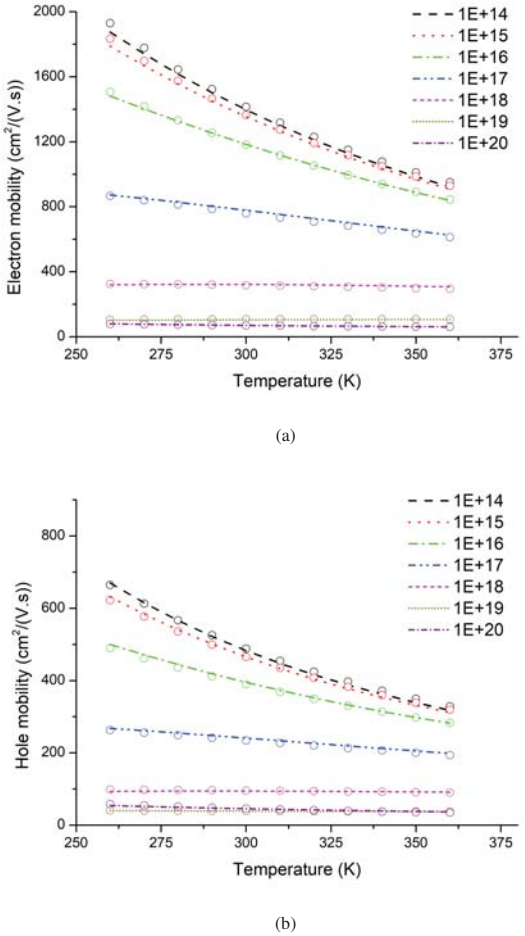

Fig. 2 Mobility temperature relation of electrons (a) and holes (b) in silicon for different doping concentrations (scatter symbols are for experiment values, lines are for simulated values)

IV. Application to Experiment Data of Polycrystalline Silicon Film

Since the deposition, doping and annealing conditions affect the structural and electrical properties of polycrystalline silicon film [22], grain size, trap density and barrier height can be influenced by processing condition. In this section, some reported and our own experiment results for both n and p-type polycrystalline silicon will be analyzed with the new relaxation time model. It can be seen that over a large doping concentration range the thermoelectric properties as a function of temperature can be properly modeled with the new model, if the physical parameters grain size, trap density and barrier height are used as fitting parameters.

The reported electrical conductivity for three samples of phosphorus doped and laser-crystallized polycrystalline silicon film [18] and one boron doped polycrystalline silicon film [10] are shown in Fig. 3 together with the fitted results. The doping concentrations of the three phosphorus doped samples are a: $7 \times 10^{19}\,cm^{-3}$, b: $3.5 \times 10^{19}\,cm^{-3}$, and c: $9 \times 10^{18}\,cm^{-3}$, respectively. The doping concentration of the boron doped sample d is $3 \times 10^{18}\,cm^{-3}$. The fitting parameters for data

presented are listed in Table I. One can see that the fitted conductivity agrees well with experiment, and the extracted grain size is also in agreement with the experiment value of $100\,nm$ to $300\,nm$.

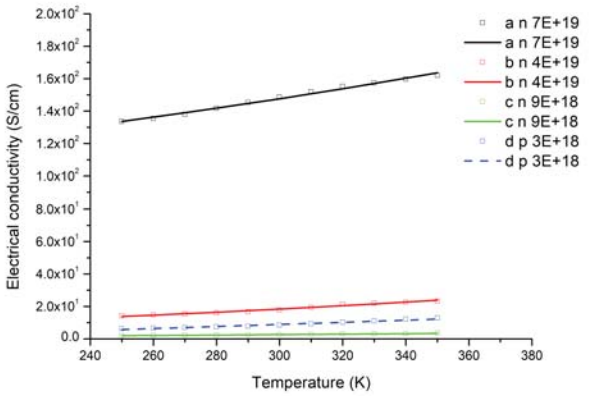

Fig. 3 The electrical conductivity as a function of temperature for three n-doped and one p-doped polycrystalline slicon films (scatter symbols are for experiment values, lines are for simulated values); experiment data are from [6]

Both electrical conductivity and Seebeck coefficient were measured for two boron doped and two phosphorus doped polycrystalline silicon samples as function of temperature [23]. In [23] the implant parameters and polycrytalline silicon film thickness are given. Since the doping will be redistributed in top and bottom oxide and there may be some out diffusion effect of dopant, it is difficult to get the doping concentration from the implant dose and film thickness along. The doping concentration should be used as fitting parameter. The reported electrical conductivity values together with the fitted results are shown in Fig. 4a. The measured and fitted Seebeck coefficient are shown in Fig. 4b. The fitting parameters are presented in Table I. The model reasonably reproduces the experiment results.

Our experiment results are also analyzed with the new relaxation time model. The experiment and simulated data are shown in Fig. 5. The fitted parameters are shown in Table I. The experiment results can also be well explained by the model.

V. Discussion

As example, the transport properties of phosphorus doped polycrystalline films as function of mean grain size are simulated with current model for doping concentration from $10^{17}\,cm^{-3}$ to $10^{20}\,cm^{-3}$ at temperature $300\,K$ in Figs. 6 and 7. Here trap density of $2\times10^{12}\,cm^{-2}$ and $\chi = 0.1\,eV$ are assumed. In comparison with energy filtering model [6], no energy cut off by the potential barrier for the carrier's contribution is assumed. Although all free carriers are taken into account (3), low energy carriers are effectively blocked by the barrier due to quantum tunnel transition. Therefore, one still observes an effective energy filtering effect (Fig. 6), which shows that the Seebeck coefficient is getting larger for

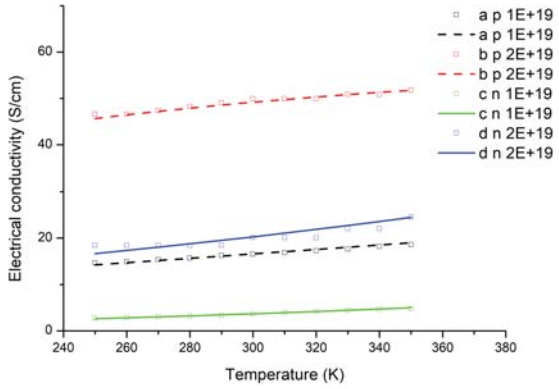

(a)

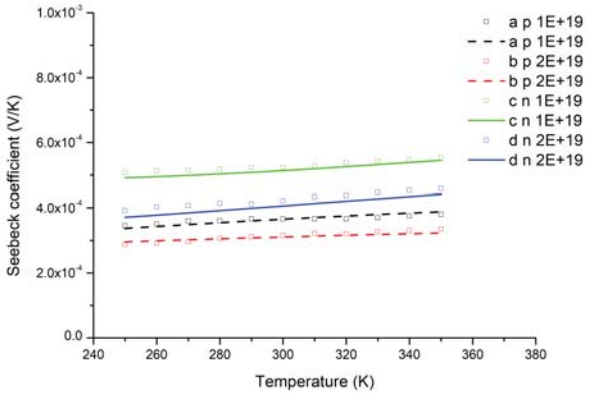

(b)

Fig. 4 The electrical conductivity (a) and Seebeck coefficient (b) as a function of temperature for two n-doped and two p-doped polycrystalline silicon films (scatter symbols are for experiment values, lines are for simulated values); experiment data are from [23]

smaller grain size due to the higher potential barrier (15). The potential barrier determined is therefore not the same as that of energy filtering model due to quantum tunnel contribution. Further, the depletion effect of grain boundary trap is seen in Fig. 7. The conductivity reduces rapidly as free carriers are trapped more in smaller grain. This agrees with the experiment observation, that the conductivity of polycrystalline silicon film experiences a sharp reduction if the doping concentration is decreased to below a critical value [4], [5]. This can also be seen in Fig. 8 for the fitting of experimentally measured conductivity with respect to doping concentration of p-type polycrystalline silicon [4]. The fitting parameters are also shown in Table I, which are supposed as the same for all distinct doping concentrations. The fitting error may be due to a possible scatter of experiment parameters, which can exist in different samples. Although the Seebeck coefficient is high for weakly doped polycrystalline silicon film, the electrical conductivity is much larger for polycrystalline silicon film with high doping concentrations. The ZT figure of merit and power factor are better for heavily doped polycrystaline silicon film,

TABLE I
PARAMETERS USED IN THE DATA PLOTS

Figure	Sample	Type	Doping conc.	Trap den. Q_t	Barrier χ	Grain size d
			cm^{-3}	cm^{-2}	eV	nm
Fig. 3	a	n	7×10^{19}	2.0×10^{13}	0.19	128
Fig. 3	b	n	3.5×10^{19}	1.6×10^{13}	0.21	108
Fig. 3	c	n	9×10^{18}	6.8×10^{12}	0.31	106
Fig. 3	d	p	3×10^{19}	4.5×10^{12}	0.05	315
Fig. 4	a	p	7×10^{18}	4.6×10^{12}	0.18	92
Fig. 4	b	p	1.2×10^{19}	7.3×10^{12}	0.06	93
Fig. 4	c	n	7×10^{18}	6.0×10^{12}	0.23	84
Fig. 4	d	n	1.2×10^{19}	6.7×10^{12}	0.21	112
Fig. 5	a	p	6.7×10^{19}	1.3×10^{13}	0.10	144
Fig. 5	b	n	1.3×10^{20}	6.7×10^{12}	0.11	143
Fig. 8		p		1.4×10^{12}	0.23	110

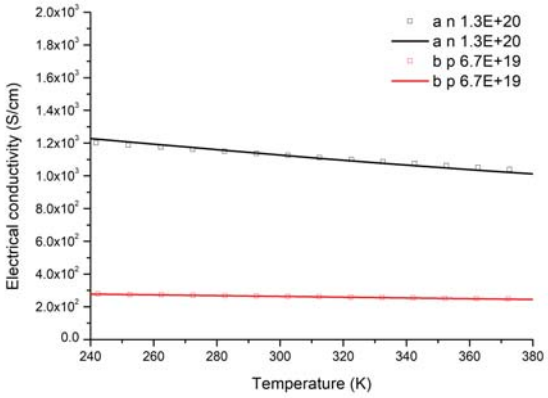

Fig. 5 The electrical conductivity as a function of temperature for one n-doped and one p-doped polycrystalline silicon film (scatter symbols are for experiment values, lines are for simulated values)

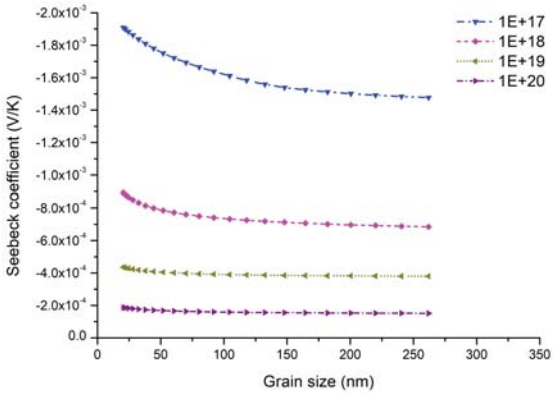

Fig. 6 The Seebeck coefficient as a function of mean grain size for four different doping concentrations at $300K$ in n-doped polycrystalline silicon

which is the reason for our experiment study of the heavily doped polycrystalline silicon film.

VI. SUMMARY

In this article, an approach for the investigation of thermoelectric properties of polycrystalline semiconductor materials is presented. The transmission probability model of charge carrier scattering at grain boundaries and trap-induced barriers was extended to a relaxation time model. This approach includes most of the important effects of phonon and charge carrier scattering at impurities, grain boundaries and grain boundary traps. The grain boundary traps induced reduction of carriers concentration is also included. It can therefore simulate electrical and thermoelectric properties simultaneously. For polycrystalline silicon, the model's parameters were discussed and fitted.

For thermoelectric applications, a polycrystalline silicon film operates in a near-equilibrium state. Furthermore, different grains and scattering centers interact independently with phonons and charge carriers. Thus, the simplified semiclassical model presented herein can give good simulation results for thermoelectric properties of polycrystalline semiconductor materials.

In order to be applicable to wider temperature ranges and to yield more quantitative descriptions, additional scattering mechanisms may have to be included, especially in nanometer grain size regime [24]. Furthermore, the effect of having distributions of grain sizes and trap energy levels may also have to be taken into account. For high doping concentrations, the influence of the tail of the energy band edge may also be non-negligible. All of the aforementioned extensions can be added to the presented model because they can be treated in a statistically independent manner.

Further experiments are needed to gain more quantitative insight about the variation of trap density, trap energy, and grain size as functions of deposition conditions, processing conditions, and the activation processes of different annealing procedures. This is required in order to make our approach more suitable for the optimization of polycrystalline silicon used for the thermoelectric devices. The approach presented herein can be extended to investigate the transport behavior of other crystalline and polycrystalline semiconductors.

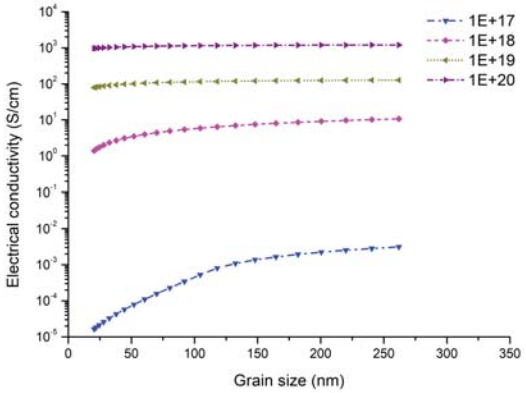

Fig. 7 The electrical conductivity as a function of mean grain size for four different doping concentrations at $300K$ in n-doped polycrystalline silicon

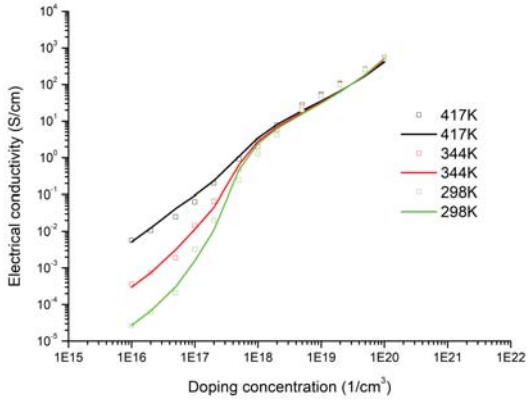

Fig. 8 The electrical conductivity as a function of doping concentration for three different temperature in p-doped polycrystalline silicon (scatter symbols are for experiment values, lines are for simulated values); experiment data are from [4]

ACKNOWLEDGMENT

Li Long thanks Dr. Torsten Sachse and Dr. Wei Long for the valuable discussions and suggestions.

REFERENCES

[1] C. Goupil, W. Seifert, K. Zabrocki, E. Müller, and G. J. Snyder, "Thermodynamics of thermoelectric phenomena and applications," *Entropy*, vol. 2011, no. 13, pp. 1481–1516, Aug. 2011.

[2] H. B. Callen, "The application of Onsager's reciprocal relations to thermoelectric, thermomagnetic, and galvanomagnetic effects," *Phys. Rev.*, vol. 73, no. 11, pp. 1349–1358, Jun. 1948.

[3] N. F. Hinsche, F. Rittweger, M. Hölzer, P. Zahn, A. Ernst, and I. Mertig, "Ab initio description of the thermoelectric properties of heterostructures in the diffusive limit of transport," *Phys. Status Solidi*, vol. A 213, no. 3, pp. 672–683, Oct. 2015.

[4] N. C.-C. Lu, L. Gerzberg, C.-Y. Lu, and J. D. Meindl, "Modeling and optimization of monolithic polycrystalline silicon resistors," *IEEE Transactions on Electron Devices*, vol. ED-28, no. 7, pp. 818–830, Jul. 1981.

[5] J. Y. W. Seto, "The electrical properties of polycrystalline silicon films," *J. Appl. Phys.*, vol. 46, no. 12, pp. 5247–5254, Dec. 1975.

[6] Y. Kajikawa, "Conduction model covering non-degenerate through degenerate polycrystalline semiconductors with non-uniform grain-boundary potential heights based on an energy filtering model," *J. Appl. Phys.*, vol. 112, no. 12, p. 123713, Dec. 2012.

[7] N. Neophytou, X. Zianni, H. Kosina, S. Frabboni, B. Lorenzi, and D. Narducci, "Simultaneous increase in electrical conductivity and seebeck coefficient in highly boron-doped nanocrystalline Si," *Nanotechnology*, vol. 24, no. 20, p. 205402, May 2013.

[8] V. Vargiamidis, M. Thesberg, and N. Neophytou, "Theoretical model for the seebeck coefficient in superlattice materials with energy relaxation," *J. Appl. Phys.*, vol. 126, no. 5, p. 055105, Aug. 2019.

[9] C. B. Vining, "A model for the high-temperature transport properties of heavily doped n-type silicon-germanium alloys," *J. Appl. Phys.*, vol. 69, no. 1, pp. 331–341, Jan. 1991.

[10] N. C.-C. Lu, L. Gerzberg, C.-Y. Lu, and J. D. Meindl, "A conduction model for semiconductor-grain-boundary-semiconductor barriers in polycrystalline-silicon films," *IEEE Transactions on Electron Devices*, vol. ED-30, no. 2, pp. 137–149, Feb. 1983.

[11] A. Popescu, L. M. Woods, J. Martin, and G. S. Nolas, "Model of transport properties of thermoelectric nanocomposite materials," *Phys. Rev. B*, vol. 79, p. 205302, May 2009.

[12] G. D. Mahan, L. Lindsay, and D. A. Broido, "The seebeck coefficient and phonon drag in silicon," *J. Appl. Phys.*, vol. 116, p. 245102, Dec. 2014.

[13] S. S. Li, *Semiconductor Physical Electrons*, 1st ed. New York, NY, USA: Plenum Press, 1993.

[14] J. Lutz, H. Schlangenotto, U. Scheuermann, and R. D. Doncker, *Semiconductor Power Devices, Physics, Characteristics, Reliability*, 1st ed. Berlin, Germany: Springer, 2011.

[15] M. Lundstrom, *Fundamentals of carrier transport*, 2nd ed. Cambridge, UK: Cambridge university press, 2000.

[16] M. V. Fischetti and S. E. Laux, "Band structure, deformation potentials, and carrier mobility in strained Si, Ge, and SiGe alloys," *J. Appl. Phys.*, vol. 80, no. 10, pp. 2234–2252, Jun. 1996.

[17] B. P. Tyagi and K. Sen, "Electrical properties of polycrystalline silicon in the dark and under illumination," *phys. stat. sol. (a)*, vol. 90, no. 2, pp. 709–713, Aug. 1985.

[18] K. v. Maydell, S. Brehme, N. H. Nickel, and W. Fuhs, "Electronic transport in P-doped laser-crystallized polycrystalline silicon," *Thin Solid Films*, vol. 487, no. 1-2, pp. 93–96, Sept. 2005.

[19] J. M. Dorkel and P. Leturcq, "Carrier mobilities in silicon semi-empirically related to temperature, doping and injection level," *Solid-State Electronics*, vol. 24, no. 9, pp. 821–825, Sep. 1981.

[20] N. Neophytou and H. Cosina, "Large enhancement in hole velocity and mobility in p-type [110] and [111] silicon nanowires by cross section scaling: An atomistic analysis," *Nano Lett.*, vol. 10, no. 12, pp. 4913–4919, Nov. 2010.

[21] Silvaco, *Athena user's manual*. Santa Clara, CA 95054: Silvaco, Inc, 2015.

[22] J. Y. W. Seto, "Deposition of polycrystalline silicon by pyrolysis of silane in argon," *J. Electrochem. Soc.: Solid-State Science and Technology*, vol. 122, no. 5, pp. 701–706, May 1975.

[23] F. Völklein and H. Baltes, "Thermoelectronic properties of polysilicon films doped with phosphorus and boron," *Sensors and Materials*, vol. 3, no. 6, pp. 325–334, Sept. 1991.

[24] N. Neophytou, S. Foster, V. Vargiamidis, G. Pennelli, and D. Narducci, "Nanostructured potential well/barrier engineering for realizing unprecedentedly large thermoelectric power factors," *Materials Today Physics*, vol. 11, p. 100159, Dec. 2019.

Li Long received the B.S. and M.S. degrees in Physics from Wuhan University, P.R. China, in 1983 and 1986, respectively, and the Ph.D degree in Physics from Technische Universität Bergakdemic Freiberg, Germany, in 2001. From 1986 to 1995 he was a lecturer at the Physics department, Wuhan University, P. R. China. From 2001 to 2002 he was a postdoc at the Faculty of Physics, Universität Halle, Germany. In 2003 he was a postdoc at the Max Planck Institute of microstructure physics, Halle, Germany. Since 2004 he has been an R&D engineer at the CiS Research Institute of Microsensors, Erfurt, Germany. His research focuses on the development of silicon microsensors. His work includes design, simulation, and analysis of thermopile sensors, photosensors and micro-strip detectors and micro-pixel detectors.

Thomas Ortlepp was born in Friedrichroda, Thuringia, in 1972 and is a trained maintenance mechanic. He studied mathematics at the Technical University of Ilmenau and received his PhD in quantum electronics in 2004. After that, Thomas Ortlepp did research in the field of low-temperature physics at the University of Twente in Holland. In 2010, Thomas Ortlepp habilitated in the field of microelectronics and subsequently took over the leadership of an industrial project for high-performance quantum memory circuits at the University of Berkeley in California. In 2013, Thomas Ortlepp returned to Germany and started his career at CiS Forschungsinstitut für Mikroelektronik GmbH. In 2015, he was appointed distinguished professor by Yokohama National University. Also in 2015, Thomas Ortlepp took over the management of the CiS Research Institute of Microsensors (CiS Forschungsinstitut für Mikroelektronik GmbH) until today. He is co-founder and vice president of the MEMS Smart Sensor Institute in Nanjing, China, which was established in 2018. His research focuses on the development of silicon microsystems (MEMS and MOEMS) and the industrial application of quantum technology.